



Published in final edited form as:

Oncogene. 2013 June 13; 32(24): 2927–2936. doi:10.1038/onc.2012.311.

Modulation of Neuroblastoma Disease Pathogenesis By An Extensive Network of Epigenetically Regulated MicroRNAs

Sudipto Das^{1,2,^}, Kenneth Bryan^{1,2,^}, Patrick G Buckley^{1,2}, Olga Piskareva^{1,2}, Isabella M Bray^{1,2}, Niamh Foley^{1,2}, Jacqueline Ryan^{1,2}, Jennifer Lynch^{1,2}, Laura Creevey^{1,2}, Joanna Fay^{1,2}, Suzanne Prenter^{1,2}, Jan Koster³, Peter van Sluis, Rogier Versteeg³, Angelika Eggert⁴, Johannes H Schulte⁴, Alexander Schramm⁴, Pieter Mesdagh⁵, Jo Vandesompele⁵, Frank Speleman⁵, and Raymond L Stallings^{1,2}

¹Department of Molecular and Cellular Therapeutics, Royal College of Surgeons in Ireland, Dublin, Ireland ²National Children's Research Centre, Our Lady's Children's Hospital, Dublin, Ireland ³Academic Medical Center, University of Amsterdam, Amsterdam, Netherlands ⁴University Children's Hospital, Essen, Germany ⁵Ghent University Hospital, Ghent, Belgium

Abstract

MicroRNAs contribute to the pathogenesis of many forms of cancer, including the pediatric cancer neuroblastoma, but the underlying mechanisms leading to altered miRNA expression are often unknown. Here, a novel integrated approach for analyzing DNA methylation coupled with miRNA and mRNA expression data sets identified 67 epigenetically regulated miRNA in neuroblastoma. A large proportion (42%) of these miRNAs were associated with poor patient survival when under-expressed in tumors. Moreover, we demonstrate that this panel of epigenetically silenced miRNAs targets a large set of genes that are over-expressed in tumors from patients with poor survival in a highly redundant manner. The genes targeted by the epigenetically regulated miRNAs are enriched for a number of biological processes, including regulation of cell differentiation. Functional studies involving ectopic over-expression of several of the epigenetically silenced miRNAs had a negative impact on neuroblastoma cell viability, providing further support to the concept that inactivation of these miRNAs is important for neuroblastoma disease pathogenesis. One locus, miR-340, induced either differentiation or apoptosis in a cell context dependent manner, indicating a tumor suppressive function for this miRNA. Intriguingly, it was determined that miR-340 is up-regulated by demethylation of an upstream genomic region that occurs during the process of neuroblastoma cell differentiation induced by all-trans retinoic acid (ATRA). Further biological studies of miR-340 revealed that it directly represses the *SOX2* transcription factor by targeting of its 3' UTR, explaining the mechanism by which *SOX2* is down-regulated by ATRA. Although *SOX2* contributes to the maintenance of stem cells in an

Users may view, print, copy, and download text and data-mine the content in such documents, for the purposes of academic research, subject always to the full Conditions of use:http://www.nature.com/authors/editorial_policies/license.html#terms

Correspondence to: Raymond L Stallings.

[^]These authors contributed equally to the work.

Supplementary Information accompanies the paper on the *Oncogene* website (<http://www.nature.com/onc>).

CONFLICT OF INTEREST

The authors declare that they have no conflict of interest.

undifferentiated state, we demonstrate that miR-340 mediated down-regulation of SOX2 is not required for ATRA induced differentiation to occur. In summary, our results exemplify the dynamic nature of the miRNA epigenome and identify a remarkable network of miRNA/mRNA interactions that significantly contribute to neuroblastoma disease pathogenesis.

Keywords

miRNA; methylation; tumor suppressor; neuroblastoma; SOX2

INTRODUCTION

MicroRNAs (miRNAs) are a well established class of small RNA sequences which down-regulate gene expression at a post-transcriptional level through targeting regions of sequence complementarity in mRNA 3' UTRs (1). The dysregulation of miRNA expression contributes to many aspects of tumor pathogenesis in virtually all forms of cancer, including the paediatric cancer neuroblastoma (2, 3), with several miRNAs having demonstrated oncogenic or tumor suppressor functions (4-12). Mechanisms leading to the dysregulation of miRNAs in these tumors involves chromosomal imbalances (13, 14), along with over-expression of the MYCN transcription factor in clinically aggressive disease subtypes (9, 13, 15, 16). Here, we investigate whether DNA hypermethylation of miRNA regulatory regions contributes towards their transcriptional silencing in neuroblastoma. The epigenetic silencing of protein coding genes is a significant mechanism of down-regulating tumor suppressor functions in these tumors (17-21), and a number of tumor suppressor miRNAs are known to be regulated by DNA methylation in other forms of cancer (22-26).

In this report, we use a novel integrated analysis approach involving DNA methylation profiling, coupled with miRNA and mRNA expression data, to identify an extensive set of epigenetically regulated miRNAs in neuroblastoma tumors. We show how this set of epigenetically regulated miRNAs targets a multitude of genes which are over-expressed in tumours from patients with poor survival with extensive redundancy. Functional analysis of ectopic over-expression of several epigenetically silenced miRNAs in neuroblastoma cell lines further supports their tumor suppressive nature.

One of the major biological processes regulated by the genes targeted by the epigenetically modulated miRNAs is cell differentiation. Differentiation is important in the treatment of high stage neuroblastoma patients as they receive 13-cis retinoic acid at the end stage of therapy to eliminate minimal residual disease, and a related compound, all-trans retinoic acid (ATRA) induces some neuroblastoma cell lines to differentiate (27). Previously, we showed that neuroblastoma cell lines treated with ATRA undergo genome-wide DNA methylation alterations at the promoter regions of functionally relevant genes as a consequence of miRNA mediated inhibition of DNA methyltransferase activity (6). Here, we demonstrate that DNA methylation changes occurring during ATRA induced differentiation also include 5' regulatory regions of tumor suppressor miRNAs. Specifically, we show that down-regulation of the SOX2 during ATRA induced differentiation is

mediated by a miRNA that is up-regulated and over-expressed as a consequence of demethylation following ATRA treatment.

Our results provide novel insight on genome-wide DNA methylation as a mechanism of silencing an extensive network of tumor suppressor miRNAs that redundantly target genes which are over-expressed in tumours from patients with poor survival.

RESULTS

Identifying epigenetically silenced miRNAs in primary neuroblastoma tumors and cell lines

Methylated DNA immunoprecipitation (MeDIP) was carried out on DNA samples isolated from 18 primary neuroblastoma tumors (Supplementary Table S1) and Kelly, SK-N-AS and SK-N-BE cells to assess the methylation status of up-stream regions of miRNAs. MeDIP enriched DNA was hybridized to custom tiling arrays spanning 50 kb up-stream and 20 kb down-stream of 528 miRNA loci. Integrated analysis was restricted to 298 miRNA loci for which qPCR expression data was available. The experimental design is presented in Figure 1a.

Analysis of DNA methylation was performed within 10 kb up-stream of each pre-miRNA based on predicted transcriptional start sites and putative promoter regions for the majority of miRNAs (28). Statistically significant DNA methylation peaks within this region were identified and the mean probe score within the region covered by the peaks was calculated for every locus in each sample, allowing quantification of DNA methylation levels. Next, we identified the DNA methylation peak mapping closest to the pre-miRNA sequence where the levels of methylation exhibited a significant inverse correlation (Spearman's $r < -0.40$, $p < 0.05$) with the expression level of the respective miRNA. In total, 67 miRNA were identified with a DNA methylation peak in which the mean methylation score was significantly inversely correlated with expression across the set of tumors (Supplementary Table S2).

Two dimensional hierarchical cluster analysis was carried out on the tumors based on both expression of the 67 methylation-sensitive miRNAs and the methylation levels of the peak mapping closest to the pre-miRNA (Figure 1b). Several studies have used the presence of histone marks or RNA polymerase II binding sites to predict the positions of miRNA transcriptional start sites (TSS) (29-32), and it is of interest that 28 (42%) of the DNA methylation peaks identified in our study either overlap or map within -2kb or +500 bp of a predicted TSS (Supplementary Table S2). In eight instances miRNA forming parts of genomic clusters had nearly identical expression patterns in the tumors, consistent with them being regulated by the same methylated up-stream site.

A recent report has shown that the majority of DNA methylation for protein coding genes occurs in regions known as CpG shores, which are regions within 2 kb of a CpG island (CGI) (33). Similar to protein coding genes, the majority of methylation peaks for miRNAs were located in CpG shores as opposed to CGI, with the frequency of methylation peaks decreasing as distance from the CGI increased (Figure 1c).

DNA methylation status was also validated for several loci in four tumors and two cell lines (Kelly and SK-N-BE) by EpiTYPER analysis which allowed quantitative assessment of methylation at selected loci. There were statistically significant ($p < 0.05$) positive correlations between the two data sets (Supplementary Figure S1).

Clinical relevance and functional validation of miRNAs regulated by DNA methylation

Remarkably, 42% ($n = 28$) of the epigenetically regulated miRNAs were significantly associated with either lower event-free (EFS) or overall (OS) patient survival when under-expressed in 237 neuroblastoma tumors (Figure 1b; Supplementary Figure S2). This represents a significant enrichment for prognostically relevant miRNA among those that are epigenetically silenced. Treatment of Kelly SK-N-AS, SHSY-5Y and SK-N-BE with the demethylating agent 5'-aza-2 deoxycytidine (5'-Aza) revealed that 30 out of the 67 miRNAs had significantly increased expression in one or more cell lines (for both biological replicates >1.5 fold increase; $p < 0.05$) (Figure 1b and Supplementary Figure S3), providing functional validation of DNA methylation as a regulatory mechanism. Among the miRNAs that were associated with poor patient survival when under-expressed in tumors, 53% (16/30) could be reactivated by 5' Aza.

The impact of ectopic over-expression of three epigenetically silenced miRNAs, miR-195, miR-196a, and miR-497 on the viability of Kelly, NB1691, SK-N-BE, or SK-N-AS neuroblastoma cells was assessed. Cell lines transfected with these miRNAs exhibited significantly decreased cell viability by 96 hours post-transfection (Supplementary Figure S4), further underscoring the importance of these miRNAs as tumor suppressors.

Although the majority of the 67 epigenetically regulated miRNAs were hypermethylated and inactivated in poor prognosis tumours, 10 were hypermethylated in favourable tumors and over-expressed in tumours from patients with poor OS/EFS (Figure 2b and Supplementary Figure S2).

Identification of gene targets of epigenetically regulated miRNA

In order to identify potential mRNA targets of the methylation sensitive miRNAs, a panel of 42 primary neuroblastoma tumors with both miRNA (TaqMan qPCR) and mRNA (Affymetrix Exon array) expression data was analyzed to identify mRNAs inversely correlated with the 67 epigenetically regulated miRNAs. In total, 1,250 mRNAs had expression patterns that were significantly inversely correlated to at least one miRNA, and had 3'UTRs that were significantly enriched for predicted target sites from the set of 55 miRNA (Supplementary Table S3). The number of miRNAs predicted to bind to an mRNA was significantly positively correlated with the level of inverse expression ($P < 2.2e^{-16}$, $r = 0.64$) (Figure 2a). For the 3' UTR of *CDK6*, four of the 16 predicted miRNA target sites (miR-29b, -29c, -195 and let-7b) have been experimentally validated in other studies (34-37).

Microarray mRNA data from an independent set of 88 tumors (<http://R2.amc.nl>) was then used to determine if the genes targeted by the miRNAs had any significant correlations with poor OS when over-expressed in tumors. Remarkably, 56% ($n = 35$) of the top 5% of our

predicted target genes were over-expressed in tumors from patients with lower OS (Figure 2a, Supplementary Table S4). In contrast, only 14% (n = 9) of genes in the bottom 5% were over-expressed in tumors from patients with lower OS (Supplementary Table S4), representing a statistically significant skewing ($p=8.8e^{-05}$). The relationships between genes from the top 5% grouping (i.e., greatest number of miRNA target sites) and the epigenetically regulated miRNAs are depicted in Figure 2b.

Gene ontology analysis carried out on the entire set of 1,250 target genes demonstrated enrichment for a number of biological processes, including regulation of cell differentiation, an effect that is induced by all-trans retinoic acid (ATRA) treatment of some neuroblastoma cell lines (Figure 2c).

ATRA treatment results in functionally significant DNA de-methylation of miRNA regulatory regions

We previously reported that neuroblastoma cell lines exhibit a substantial de-methylation of promoter regions for protein coding genes following ATRA treatment (6), leading us to consider the possibility that similar epigenetic alterations might occur at promoter regions of miRNAs. MeDIP microarray analysis, along with miRNA expression analysis was carried out on ATRA treated and untreated SK-N-BE cells. Twenty miRNAs had up-stream regions (<10 kb from the pre-miRNA) which were de-methylated and up-regulated >1.5 fold ($p<0.05$) following ATRA treatment. Twenty-four miRNAs were hypermethylated and down-regulated >1.5 fold post-ATRA treatment. Analysis of miRNA expression in an independent cell line (SHSY-5Y) following ATRA treatment indicated that four of the de-methylated miRNAs and nine of the hypermethylated were over or under-expressed following 7 days of ATRA exposure, respectively, indicating that some of the methylation changes are a consistent feature of differentiation. None of the hypermethylated miRNAs were correlated with patient EFS or OS, and among the de-methylated miRNAs, only miR-340 was significantly re-expressed in both cell lines following ATRA treatment (Figure 3a). This miRNA was also significantly associated with poor OS and EFS when under-expressed in 237 primary NB tumors (Figure 3b, c). There were four distinct methylation peaks (Figure 3d) within 10 kb up-stream of miR-340, with all peaks having varying levels of de-methylation in response to ATRA treatment. miR-340 was identified as an epigenetically regulated miRNA in primary tumors (Figure 1b) and was significantly up-regulated after 5'-Aza treatment in both SK-N-BE and SHSY-5Y (Figure 1b and Supplementary Figure S3).

Functional effects of miR-340 over-expression

Given that miR-340 is functionally inactivated by DNA methylation in neuroblastoma, mature miR-340 mimics or a negative control were transfected into SK-N-BE, SHSY-5Y and Kelly cells to elucidate the biological effects. Following transfection, over-expression of miR-340 was validated by qPCR (Supplementary Figure S5). miR-340 over-expression resulted in a significant reduction in cell viability for each cell line (Figure 4a), and also significantly impeded colony forming ability (Figure 4b).

miR-340 was up-regulated in SK-N-BE and SHSY-5Y following ATRA treatment, but not in Kelly. It is intriguing that the phenotypic response of Kelly cells to ATRA is apoptosis (38), while both SK-N-BE and SHSY-5Y are well known to undergo neural differentiation. We therefore decided to test the hypothesis that ectopic over-expression of miR-340 has different phenotypic consequences in these cell lines. As illustrated in Supplementary Figure S6a, miR-340 over-expression in Kelly resulted in the cells becoming rounded and detached. A significant increase in apoptosis was confirmed by FACS analysis of P.I./annexin V stained cells (Supplementary Figure S6b,c). In contrast, SK-N-BE cells at 7 days post miR-340 transfection had increased neurite extensions (Supplementary Figure S7a) and miR-340 transfection yielded no change in the number of apoptotic cells relative to the negative control (Supplementary Figure S7b,c). PI staining followed by FACS analysis of SK-N-BE cells transfected with miR-340 or negative control sequences revealed an accumulation of cells in S-phase and a significant decrease in the G2-phase of the cell cycle ($p=0.03$) at 96-hours post-transfection (Figure 4c), indicating a block during S-phase. The expression of three markers of differentiation (*SOX2*, *PAX6* and *TUBB3*) at 7 days post miR-340 transfection of SK-N-BE and SHSY-5Y cells was also assessed. Consistent with ATRA induced differentiation, both *SOX2* and *PAX6* had significantly decreased mRNA levels in the transfected cells at 7 days post miR-340 transfection (Supplementary Figure S8a,b). However, there was no change in the levels of *TUBB3* at this time point in either cell lines (Supplementary Figure S8c). Interestingly, *SOX2* over-expression in the $n = 88$ tumor set is significant for poor OS and EFS with one probe (Supplementary Figure S8d,e), consistent with findings at protein level (39).

miR-340 directly targets the 3'-UTR of *SOX2* transcription factor

As described in the preceding section, *SOX2* mRNA was down-regulated at 7 days post miR-340 transfection (Supplementary Figure S8a). *SOX2* was also determined to be significantly down-regulated at 3 days post miR-340 transfection at mRNA (Figure 5a) and protein level (Figure 5c). The down-regulation of *SOX2* in ATRA treated cells (Figure 5b) is inversely correlated with the up-regulation of miR-340 (Figure 3a). As a potential explanation for this inverse relationship, we determined that the 3'-UTR of *SOX2* contained three predicted miR-340 binding sites (TargetScan) (Figure 5d).

To validate miR-340 targeting of *SOX2*, we cloned the complete 1.1 kb 3' UTR of *SOX2* into a luciferase reporter vector, psi-CHECK2. Co-transfection of miR-340 mimics and psi-CHECK2-*SOX2*-3'UTR significantly reduced luciferase activity, and mutation of all three miR-340 binding sites abrogated the negative effect of miR-340 on luciferase activity (Figure 5e). The mutation of individual binding sites did not abrogate the effects of miR-340 on luciferase expression, and two of the three double mutant constructs failed to diminish luciferase activity. However, the mutation of binding sites 2192 and 2137, with binding site 1910 remaining active, abolished the effect of miR-340 on luciferase activity, similar to the triple deletion mutant, indicating that the 1910 binding site has no functional effect. We conclude that miR-340 directly targets two binding sites in the *SOX2* 3' UTR.

In order to confirm if the up-regulation of miR-340 is responsible for the down-regulation of *SOX2* in response to ATRA, a locked nucleic acid (LNA) antisense-miR-340 sequence was

transfected into SK-N-BE cells 24 hours prior to ATRA treatment, resulting in a substantial reduction in miR-340 (Supplementary Figure S9a) and an increase in SOX2 protein levels within 96 hours post-ATRA treatment (Supplementary Figure S9b). SK-N-BE cells with increased SOX2 levels had extensive neurite outgrowth within 5 days after ATRA treatment (Supplementary Figure S9c) and exhibited a decrease in cell growth that was comparable to negative controls (Supplementary Figure S9d). We conclude that up-regulation of miR-340 is responsible for reducing SOX2 levels during ATRA induced differentiation of SK-N-BE cells, but that the maintenance of SOX2 protein levels is insufficient to block differentiation from occurring.

DISCUSSION

This study is the first attempt to investigate DNA methylation as a possible mechanism for the dysregulation of miRNA expression in neuroblastoma. Our integrated analysis of DNA methylation with miRNA and mRNA expression data sets permitted the identification of a large set of epigenetically regulated miRNAs with significantly enriched target sites in the 3' UTRs of genes over-expressed in unfavourable tumor subtypes. This integrated approach identified miRNAs which have never been associated with DNA methylation (n = 41), along with 26 miRNAs that were previously validated as epigenetically regulated in other forms of cancer, as summarized in review articles (24, 26). Overall, 22% (67/298) of the miRNAs examined in our study were sensitive to the effects of DNA methylation. Dudzic *et al.* demonstrated that hypermethylation of miRNAs in bladder cancer is more frequent in CpG shores than CpG islands (40), and our results in neuroblastoma are consistent with this finding.

Our results establish that multiple epigenetically regulated miRNAs often target the same mRNA at a higher than expected frequency, indicating significant targeting redundancy. mRNAs that are targeted by multiple miRNAs exhibited more pronounced inverse expressional correlations with the targeting miRNAs, thus confirming this relationship at a functional level. This is consistent with experimental findings that targeting of mRNAs by more than one miRNA can have an additive or even a synergistic impact on reducing mRNA levels (41, 42). It should be noted that a microarray based approach will not detect miRNA/mRNA interactions that result in translational inhibition without mRNA degradation. However, some groups have reported that miRNA/mRNA interactions that result in mRNA degradation have a greater negative impact on protein levels than do interactions resulting only in translational inhibition (43, 44).

Remarkably, a high proportion of both the methylated miRNAs (42%) and their associated mRNA targets (56% of the highly redundantly targeted mRNAs) are highly associated with poor clinical outcome when under and over-expressed in tumors, respectively. Thus, a relatively high proportion of epigenetically inactivated miRNAs and their mRNA targets show promise as prognostic candidate clinical markers. Prior functional studies have indicated that several of the hypemethylated miRNAs, including miR-let-7, 10a, -10b, -101, -184, -335, and -542-5p negatively impact neuroblastoma cell viability or migration, both *in vitro* and *in vivo* (4, 5, 7, 8, 11, 45, 46). As demonstrated in this report, epigenetically silenced miR-340, -195, -196a, and -497 negatively impact neuroblastoma cell viability

when ectopically over-expressed in cell lines. Many of the genes targeted by the epigenetically regulated miRNA panel have known oncogenic functions in either neuroblastoma or other forms of cancer. For example, *AKT2* is predicted to be targeted by 9 epigenetically regulated miRNAs and the importance of *AKT2* expression for neuroblastoma cell survival has been previously demonstrated (5, 8, 11). *LIN28B*, a well established oncogene that promotes cell transformation (47, 48), is a predicted target of 9 epigenetically regulated miRNAs. *CDK6* over-expression is important in many cancers and had 16 predicted target sites from the miRNAs.

The direct targeting of *SOX2* by miR-340 has been demonstrated in this report. SRY box containing (SOX) transcription factor family members act sequentially in regulating the maintenance and differentiation of neural progenitor cells. Bergsland et al (49) demonstrated that both *SOX2* and *SOX3* pre-bind many genes in embryonic stem cells and neural progenitor cells, which can only be activated by binding of *SOX11* at a later developmental stage. In response to ATRA, *SOX2* levels decrease while *SOX3* and *SOX11* levels increase (49, 50). Here, we demonstrate that the decrease in *SOX2* expression is mediated by miR-340 targeting. Although *SOX2* is vital to maintaining normal stem cells and cancer stem cells in an undifferentiated state (50, 51), and can restore stem cell properties when co-transfected with other transcription factors into a variety of mature cell types (52), we demonstrate that a decrease in *SOX2* levels is not sufficient to deter ATRA induced differentiation of neuroblastoma cells. This is not surprising given the very large number of miRNAs and genes whose transcript levels are altered in response to ATRA. In contrast, Jankowski *et al* demonstrated that *SOX11* expression is required for neurite outgrowth and survival of murine Neuro2a following ATRA treatment (49). siRNA inhibition of these cells in the absence of ATRA also increased apoptotic cell death. This is consistent with our finding that *SOX11* is over-expressed in unfavourable tumour subtypes, and provides a rationale for why 13 miRNAs targeting this mRNA sequence are inactivated by DNA methylation.

miR-340 regulates a very large number of target mRNA sequences, so it seems likely that the impact of ectopic-over expression of miR-340 on neuroblastoma cell differentiation and apoptosis is not mediated solely through *SOX2* targeting. The pleiotropic effects of miR-340 is supported by the fact that over-expression causes SK-N-BE and SHSY-5Y cells to differentiate, and Kelly cells to undergo apoptosis. miR340 also has an impact on breast cancer cell migration and invasion through targeting the *MET* oncogene, indicating that it is a tumor suppressor of broad importance in multiple forms of cancer (53).

In summary, our findings support extensive epigenetic silencing of miRNAs that target a large repertoire of genes that are over-expressed in unfavourable neuroblastoma tumours with substantial redundancy. Our study also underscores the significance of cross talk between these miRNAs and epigenetic regulatory mechanisms in the process of neuroblastoma cell differentiation.

MATERIALS AND METHODS

Cell culture and drug treatments

SK-N-BE, SHSY-5Y, SK-N-AS and Kelly were obtained from the American Type Culture Collection and cultured under conditions recommended by the supplier. NB1691 cells were obtained from Dr. Andrew Davidoff (Memphis, TN). 5 μ mol ATRA (Sigma) was administered as described (6). Cell lines were treated with 2 μ g/ml 5-aza-2'-deoxycytidine (Sigma-Aldrich, Arklow, Ireland) for 72 hours with replenishment of media after 48 hrs. All cell lines were authenticated by STR genotyping.

Neuroblastoma tumor samples

Associations of miRNA expression with OS or EFS were performed on 237 tumors from Centres in Dublin (n=45), Ghent (n=39), Essen (n=55), and the Children's Oncology Group (n=98). The set included 52 with *MYCN* amplification and 76 with 11q loss. Disease stages included stage 4 (n=109), stage 3 (n=43), stage 2 (n=41), stage 1 (n=25) and stage 4S (n=19), while 172 patients were >1.0 years of age at diagnosis and 65 <1.0. miRNA profiling has been reported (13, 15, 16). A subgroup of tumors was used for the methylation analysis (Supplementary Table S1) and for integrated analysis of miRNA (TaqMan qPCR) and mRNA expression (Affymetrix Exon arrays). The Exon array data has been deposited in the MIAME express data repository (<http://www.ebi.ac.uk/miamexpress/cgi-bin/mx.cgi>) Accession number: E-MEXP-3517. Associations between gene expression and patient survival were identified using an independent set of 88 tumors (<http://R2.amc.nl>).

Methylated DNA immunoprecipitation (MeDIP)

MeDIP analysis was carried out for the neuroblastoma tumors and cell lines as previously described (17, 54). MeDIP and input DNA were hybridized to custom designed miRNA tiling arrays as per the manufacturer's instructions (Roche NimbleGen, Madison, WI). MeDIP microarray data on all tumors and cell lines has been deposited in the MIAME express data repository (<http://www.ebi.ac.uk/miamexpress/cgi-bin/mx.cgi>) Accession number: E-MEXP-3498.

DNA methylation validation using Sequenom EpiTYPER mass spectroscopy

Selected regions displaying differential methylation in MeDIP data were validated using Sequenom EpiTYPER mass spectroscopy analysis of bisulfite converted DNA (55) (Sequenom, Hamburg, Germany). Methylated and unmethylated control DNA was used to determine the efficiency of the EpiTYPER validation. The primer sets are provided in Supplementary Table S5.

MicroRNA transfections

MiRNA mimics (30 nmol) and the Pre-miR negative control (Applied Biosystems, Foster City, CA) were transfected into cells (3×10^5 cells/ml) using a reverse transfection method with siPORT NeoFX (Ambion, Austin, TX). Total RNA was extracted using mirNeasy Kit Qiagen, Crawley, U.K. The LNA anti-sense miR-340 probe was obtained from Exiqon (Copenhagen, Denmark).

Reverse transcription and RT-qPCR

RT-qPCR was carried out using 20 ng (miRNA expression) and 50 ng (mRNA expression) of total RNA with High-Capacity Reverse Transcription Kit (Applied Biosystems ABI). ABI TaqMan assays included: *SOX2*-Hs01053049_s1; *TUBB3*-Hs00964965; *PAX6*-Hs01088112_m1; *18s*-Hs999999901_s1; miR-340-002258; RNU66-001002. All gene expression assays and miRNA expression assays were normalized to 18s and RNU66 respectively. A relative fold change was calculated using the comparative threshold method (2^{-CT}). miRNA Taqman low-density arrays were used to carry out miRNA expression profiling for 5'-Aza and ATRA treated samples (13).

Western Blot

Western blot analysis was carried out as described (6). The membrane was probed with 1:1000 anti-SOX2 (Abcam:ab59776, Cambridge, MA) and 1:5000 anti- alpha-tubulin (Abcam:ab7291). Secondary antibodies used were 1:3000 ant-rabbit for SOX2 (ab6721) and 1:3000 anti-mouse for alpha-tubulin (ab6728).

Cell viability assays

Cell viability after miRNA transfections was assessed using either an acid-phosphatase (6). Cell viability was measured using Cell Titre 96 Aqueous One Solution Cell Proliferation Assay (Promega, Madison, WI).

Clonogenic Assay

A clonogenic assay was performed using modified protocol as described (56). 500 cells were seeded per well of a 6-well plate, 24 hours post-transfection with the miRNA mimics and negative control. Colonies were allowed to form for two weeks and then fixed using methanol and stained with crystal violet.

Cell Cycle and apoptosis analysis

Cells were harvested 96 hrs post-transfection with the miRNA mimics or negative control and subsequently fixed using 70% ethanol. The fixed cells were stained using PI/triton X-100/RNase solution and the cells were FACS sorted using the BD LSR-II Analyzer (Becton, Dickinson and Company, NJ, USA). Cell cycle analysis was performed using the FlowJo tool (<http://www.flowjo.com/index.php>). Apoptosis was measured using ANNEXIN V staining (8).

Cloning of 3'-UTR of SOX2 and luciferase assays

A 1.1 kb DNA fragment containing the entire *SOX2* 3'UTR was PCR amplified from genomic DNA using flanking primers (Supplementary Table S6), cloned into the pCR4-TOPO vector (Invitrogen, Grand Island, NY), and subsequently sub-cloned into psiCHECK2 vector (Promega) to generate psi-SOX2-3'UTR. The resultant clone was sequenced verified (GeneBank Accession No:JQ231229) and used to create the deletion mutants for miR-340 binding sites using the GeneTailor mutagenesis system (Invitrogen). Luciferase assays were performed as previously reported (8).

Integration of miRNA expression and methylation data

Discrete genomic regions prone to methylation (having a peak in at least one sample) were selected. The mean probe score across these regions was used to indicate the methylation level at that location in each sample. This enabled the study to focus on all regions that undergo methylation in neuroblastoma as opposed to solely CpG Islands. 67 miRNAs with expression significantly inversely correlated (Spearman) to peaks 10kb up-stream were selected. Two-way hierarchical clustering was performed using the integrated (additive) methylation and expression similarity matrix (see Supplementary Figure S8). In the heatmap high expression and low methylation of a miRNA is coloured red (*vice versa* green); a conflict where both are high or low is coloured black.

Target prediction of methylation sensitive miRNAs

An integrated matrix was compiled of 56 miRNAs (56/67 expressed in 10 samples) and all mRNAs that had significant inverse correlation (over 42 matched tumor samples) and a predicted 3'UTR binding site (TargetScan v5.1). mRNAs with significant over-representation of predicted target sites (Chi-square) were retained (thus nullifying biases such as 3'UTR length). The bipartite network graph in Figure 2b was generated using *Java* software package *jgraphx* v1.8.5.

Statistical analysis

Experimental miRNA data presented are based on mean replicate values and error bars indicate either standard deviation or the standard error of mean. Statistical tests used include: two-tailed, unpaired T-test, Spearman's Rank correlation and Pearson's correlation. Statistics, clustering, heatmap and scatter plots were generated by R statistical programming language v2.13.0. Kaplan Meier plots were generated using the median or quartile split and the log rank test using the R2 database (<http://R2.amc.nl/>).

Supplementary Material

Refer to Web version on PubMed Central for supplementary material.

Acknowledgments

This work was supported by grants from Science Foundation Ireland (07/IN.1/B1776), Children's Medical and Research Foundation and NIH (5R01CA127496).

References

1. He L, Hannon GJ. MicroRNAs: small RNAs with a big role in gene regulation. *Nat Rev Genet.* 2004; 5:522–31. [PubMed: 15211354]
2. Stallings RL, Foley NH, Bryan K, Buckley PG, Bray I. Therapeutic targeting of miRNAs in neuroblastoma. *Expert Opin Ther Targets.* 2010; 14:951–62. [PubMed: 20658962]
3. Stallings RL, Foley NH, Bray IM, Das S, Buckley PG. MicroRNA and DNA methylation alterations mediating retinoic acid induced neuroblastoma cell differentiation. *Semin Cancer Biol.* 2011
4. Bray I, Tivnan A, Bryan K, Foley NH, Watters KM, Tracey L, et al. MicroRNA-542-5p as a novel tumor suppressor in neuroblastoma. *Cancer Lett.* 2011; 303:56–64. [PubMed: 21310526]

5. Chen Y, Stallings RL. Differential patterns of microRNA expression in neuroblastoma are correlated with prognosis, differentiation, and apoptosis. *Cancer Res.* 2007; 67:976–83. [PubMed: 17283129]
6. Das S, Foley N, Bryan K, Watters KM, Bray I, Murphy DM, et al. MicroRNA mediates DNA demethylation events triggered by retinoic acid during neuroblastoma cell differentiation. *Cancer Res.* 2010; 70:7874–81. [PubMed: 20841484]
7. Foley NH, Bray I, Watters KM, Das S, Bryan K, Bernas T, et al. MicroRNAs 10a and 10b are potent inducers of neuroblastoma cell differentiation through targeting of nuclear receptor corepressor 2. *Cell Death Differ.* 2011; 18:1089–98. [PubMed: 21212796]
8. Foley NH, Bray IM, Tivnan A, Bryan K, Murphy DM, Buckley PG, et al. MicroRNA-184 inhibits neuroblastoma cell survival through targeting the serine/threonine kinase AKT2. *Mol Cancer.* 2010; 9:83. [PubMed: 20409325]
9. Fontana L, Fiori ME, Albin S, Cifaldi L, Giovinazzi S, Forloni M, et al. Antagomir-17-5p abolishes the growth of therapy-resistant neuroblastoma through p21 and BIM. *PLoS One.* 2008; 3:e2236. [PubMed: 18493594]
10. Mestdagh P, Bostrom AK, Impens F, Fredlund E, Van Peer G, De Antonellis P, et al. The miR-17-92 microRNA cluster regulates multiple components of the TGF-beta pathway in neuroblastoma. *Mol Cell.* 2011; 40:762–73. [PubMed: 21145484]
11. Tivnan A, Foley NH, Tracey L, Davidoff AM, Stallings RL. MicroRNA-184-mediated inhibition of tumour growth in an orthotopic murine model of neuroblastoma. *Anticancer Res.* 2011; 30:4391–5. [PubMed: 21115884]
12. Welch C, Chen Y, Stallings RL. MicroRNA-34a functions as a potential tumor suppressor by inducing apoptosis in neuroblastoma cells. *Oncogene.* 2007; 26:5017–22. [PubMed: 17297439]
13. Bray I, Bryan K, Prenter S, Buckley PG, Foley NH, Murphy DM, et al. Widespread dysregulation of miRNAs by MYCN amplification and chromosomal imbalances in neuroblastoma: association of miRNA expression with survival. *PLoS One.* 2009; 4:e7850. [PubMed: 19924232]
14. Buckley PG, Alcock L, Bryan K, Bray I, Schulte JH, Schramm A, et al. Chromosomal and microRNA expression patterns reveal biologically distinct subgroups of 11q- neuroblastoma. *Clin Cancer Res.* 2010; 16:2971–8. [PubMed: 20406844]
15. Mestdagh P, Fredlund E, Pattyn F, Schulte JH, Muth D, Vermeulen J, et al. MYCN/c-MYC-induced microRNAs repress coding gene networks associated with poor outcome in MYCN/c-MYC-activated tumors. *Oncogene.* 2010; 29:1394–404. [PubMed: 19946337]
16. Schulte JH, Schowe B, Mestdagh P, Kaderali L, Kalaghatgi P, Schlierf S, et al. Accurate prediction of neuroblastoma outcome based on miRNA expression profiles. *Int J Cancer.* 2010; 127:2374–85. [PubMed: 20473924]
17. Buckley PG, Das S, Bryan K, Watters KM, Alcock L, Koster J, et al. Genome-wide DNA methylation analysis of neuroblastic tumors reveals clinically relevant epigenetic events and large-scale epigenomic alterations localized to telomeric regions. *Int J Cancer.* 2010; 128:2296–305. [PubMed: 20669225]
18. Decock A, Ongenaert M, Vandesompele J, Speleman F. Neuroblastoma epigenetics: From candidate gene approaches to genome-wide screenings. *Epigenetics.* 2011; 6:962–70. [PubMed: 21725203]
19. Hoebeeck J, Michels E, Pattyn F, Combaret V, Vermeulen J, Yigit N, et al. Aberrant methylation of candidate tumor suppressor genes in neuroblastoma. *Cancer Lett.* 2009; 273:336–46. [PubMed: 18819746]
20. Yang Q, Kiernan CM, Tian Y, Salwen HR, Chlenski A, Brumback BA, et al. Methylation of CASP8, DCR2, and HIN-1 in neuroblastoma is associated with poor outcome. *Clin Cancer Res.* 2007; 13:3191–7. [PubMed: 17545522]
21. Yang Q, Liu S, Tian Y, Hasan C, Kersey D, Salwen HR, et al. Methylation-associated silencing of the heat shock protein 47 gene in human neuroblastoma. *Cancer Res.* 2004; 64:4531–8. [PubMed: 15231663]
22. Chim CS, Wong KY, Qi Y, Loong F, Lam WL, Wong LG, et al. Epigenetic inactivation of the miR-34a in hematological malignancies. *Carcinogenesis.* 2010; 31:745–50. [PubMed: 20118199]

23. Lodygin D, Tarasov V, Epanchintsev A, Berking C, Knyazeva T, Korner H, et al. Inactivation of miR-34a by aberrant CpG methylation in multiple types of cancer. *Cell Cycle*. 2008; 7:2591–600. [PubMed: 18719384]
24. Lopez-Serra P, Esteller M. DNA methylation-associated silencing of tumor-suppressor microRNAs in cancer. *Oncogene*. 2011
25. Vogt M, Munding J, Gruner M, Liffers ST, Verdoodt B, Hauk J, et al. Frequent concomitant inactivation of miR-34a and miR-34b/c by CpG methylation in colorectal, pancreatic, mammary, ovarian, urothelial, and renal cell carcinomas and soft tissue sarcomas. *Virchows Arch*. 2011; 458:313–22. [PubMed: 21225432]
26. Kunej T, Godnic I, Ferdin J, Horvat S, Dovc P, Calin GA. Epigenetic regulation of microRNAs in cancer: An integrated review of literature. *Mutat Res*. 2011; 717:77–84. [PubMed: 21420983]
27. Sidell N. Retinoic acid-induced growth inhibition and morphologic differentiation of human neuroblastoma cells in vitro. *J Natl Cancer Inst*. 1982; 68:589–96. [PubMed: 7040765]
28. Saini HK, Griffiths-Jones S, Enright AJ. Genomic analysis of human microRNA transcripts. *Proc Natl Acad Sci U S A*. 2007; 104:17719–24. [PubMed: 17965236]
29. Corcoran DL, Pandit KV, Gordon B, Bhattacharjee A, Kaminski N, Benos PV. Features of mammalian microRNA promoters emerge from polymerase II chromatin immunoprecipitation data. *PLoS One*. 2009; 4:e5279. [PubMed: 19390574]
30. Marson A, Levine SS, Cole MF, Frampton GM, Brambrink T, Johnstone S, et al. Connecting microRNA genes to the core transcriptional regulatory circuitry of embryonic stem cells. *Cell*. 2008; 134:521–33. [PubMed: 18692474]
31. Oszolak F, Poling LL, Wang Z, Liu H, Liu XS, Roeder RG, et al. Chromatin structure analyses identify miRNA promoters. *Genes & development*. 2008; 22:3172–83. [PubMed: 19056895]
32. Fujita S, Iba H. Putative promoter regions of miRNA genes involved in evolutionarily conserved regulatory systems among vertebrates. *Bioinformatics*. 2008; 24:303–8. [PubMed: 18055479]
33. Irizarry RA, Ladd-Acosta C, Wen B, Wu Z, Montano C, Onyango P, et al. The human colon cancer methylome shows similar hypo- and hypermethylation at conserved tissue-specific CpG island shores. *Nat Genet*. 2009; 41:178–86. [PubMed: 19151715]
34. Garzon R, Heaphy CE, Havelange V, Fabbri M, Volinia S, Tsao T, et al. MicroRNA 29b functions in acute myeloid leukemia. *Blood*. 2009; 114:5331–41. [PubMed: 19850741]
35. Johnson CD, Esquela-Kerscher A, Stefani G, Byrom M, Kelnar K, Ovcharenko D, et al. The let-7 microRNA represses cell proliferation pathways in human cells. *Cancer Res*. 2007; 67:7713–22. [PubMed: 17699775]
36. Xu T, Zhu Y, Xiong Y, Ge YY, Yun JP, Zhuang SM. MicroRNA-195 suppresses tumorigenicity and regulates G1/S transition of human hepatocellular carcinoma cells. *Hepatology*. 2009; 50:113–21. [PubMed: 19441017]
37. Zhao JJ, Lin J, Lwin T, Yang H, Guo J, Kong W, et al. microRNA expression profile and identification of miR-29 as a prognostic marker and pathogenetic factor by targeting CDK6 in mantle cell lymphoma. *Blood*. 2010; 115:2630–9. [PubMed: 20086245]
38. Girgert R, Schweizer P. Regulation of expression of two different transcripts of the NF-1 gene in neuroblastoma. *Journal of neuro-oncology*. 1997; 31:93–7. [PubMed: 9049834]
39. Gomez-Mateo Mdel C, Piqueras M, Pahlman S, Noguera R, Navarro S. Prognostic value of SOX2 expression in neuroblastoma. *Genes Chromosomes Cancer*. 2011; 50:374–7. [PubMed: 21305642]
40. Dudzic E, Miah S, Choudhry HM, Owen HC, Blizard S, Glover M, et al. Hypermethylation of CpG islands and shores around specific microRNAs and mirtrons is associated with the phenotype and presence of bladder cancer. *Clin Cancer Res*. 2010; 17:1287–96. [PubMed: 21138856]
41. Grimson A, Farh KK, Johnston WK, Garrett-Engele P, Lim LP, Bartel DP. MicroRNA targeting specificity in mammals: determinants beyond seed pairing. *Mol Cell*. 2007; 27:91–105. [PubMed: 17612493]
42. Saetrom P, Heale BS, Snove O Jr, Aagaard L, Alluin J, Rossi JJ. Distance constraints between microRNA target sites dictate efficacy and cooperativity. *Nucleic Acids Res*. 2007; 35:2333–42. [PubMed: 17389647]
43. Baek D, Villen J, Shin C, Camargo FD, Gygi SP, Bartel DP. The impact of microRNAs on protein output. *Nature*. 2008; 455:64–71. [PubMed: 18668037]

44. Guo H, Ingolia NT, Weissman JS, Bartel DP. Mammalian microRNAs predominantly act to decrease target mRNA levels. *Nature*. 2010; 466:835–40. [PubMed: 20703300]
45. Buechner J, Tomte E, Haug BH, Henriksen JR, Lokke C, Flaegstad T, et al. Tumour-suppressor microRNAs let-7 and mir-101 target the proto-oncogene MYCN and inhibit cell proliferation in MYCN-amplified neuroblastoma. *Br J Cancer*. 2011; 105:296–303. [PubMed: 21654684]
46. Lynch J, Fay J, Meehan M, Bryan K, Watters KM, Murphy DM, et al. MiRNA-335 suppresses neuroblastoma cell invasiveness by direct targeting of multiple genes from the non-canonical TGF-beta signalling pathway. *Carcinogenesis*. 2012; 33:976–85. [PubMed: 22382496]
47. Viswanathan SR, Powers JT, Einhorn W, Hoshida Y, Ng TL, Toffanin S, et al. Lin28 promotes transformation and is associated with advanced human malignancies. *Nat Genet*. 2009; 41:843–8. [PubMed: 19483683]
48. Wang YC, Chen YL, Yuan RH, Pan HW, Yang WC, Hsu HC, et al. Lin-28B expression promotes transformation and invasion in human hepatocellular carcinoma. *Carcinogenesis*. 2010; 31:1516–22. [PubMed: 20525879]
49. Jankowski MP, Cornuet PK, McIlwrath S, Koerber HR, Albers KM. SRY-box containing gene 11 (Sox11) transcription factor is required for neuron survival and neurite growth. *Neuroscience*. 2006; 143:501–14. [PubMed: 17055661]
50. Stevanovic M. Modulation of SOX2 and SOX3 gene expression during differentiation of human neuronal precursor cell line NTERA2. *Mol Biol Rep*. 2003; 30:127–32. [PubMed: 12841584]
51. Gangemi RM, Griffero F, Marubbi D, Perera M, Capra MC, Malatesta P, et al. SOX2 silencing in glioblastoma tumor-initiating cells causes stop of proliferation and loss of tumorigenicity. *Stem Cells*. 2009; 27:40–8. [PubMed: 18948646]
52. Patel M, Yang S. Advances in reprogramming somatic cells to induced pluripotent stem cells. *Stem Cell Rev*. 2010; 6:367–80. [PubMed: 20336395]
53. Wu ZS, Wu Q, Wang CQ, Wang XN, Huang J, Zhao JJ, et al. miR-340 inhibition of breast cancer cell migration and invasion through targeting of oncoprotein c-Met. *Cancer*. 2011; 117:2842–52. [PubMed: 21692045]
54. Murphy DM, Buckley PG, Bryan K, Das S, Alcock L, Foley NH, et al. Global MYCN transcription factor binding analysis in neuroblastoma reveals association with distinct E-box motifs and regions of DNA hypermethylation. *PLoS One*. 2009; 4:e8154. [PubMed: 19997598]
55. Ehrich M, Nelson MR, Stanssens P, Zabeau M, Liloglou T, Xinarianos G, et al. Quantitative high-throughput analysis of DNA methylation patterns by base-specific cleavage and mass spectrometry. *Proc Natl Acad Sci U S A*. 2005; 102:15785–90. [PubMed: 16243968]
56. Franken NA, Rodermond HM, Stap J, Haveman J, van Bree C. Clonogenic assay of cells in vitro. *Nat Protoc*. 2006; 1:2315–9. [PubMed: 17406473]

Author Manuscript

Author Manuscript

Author Manuscript

Author Manuscript

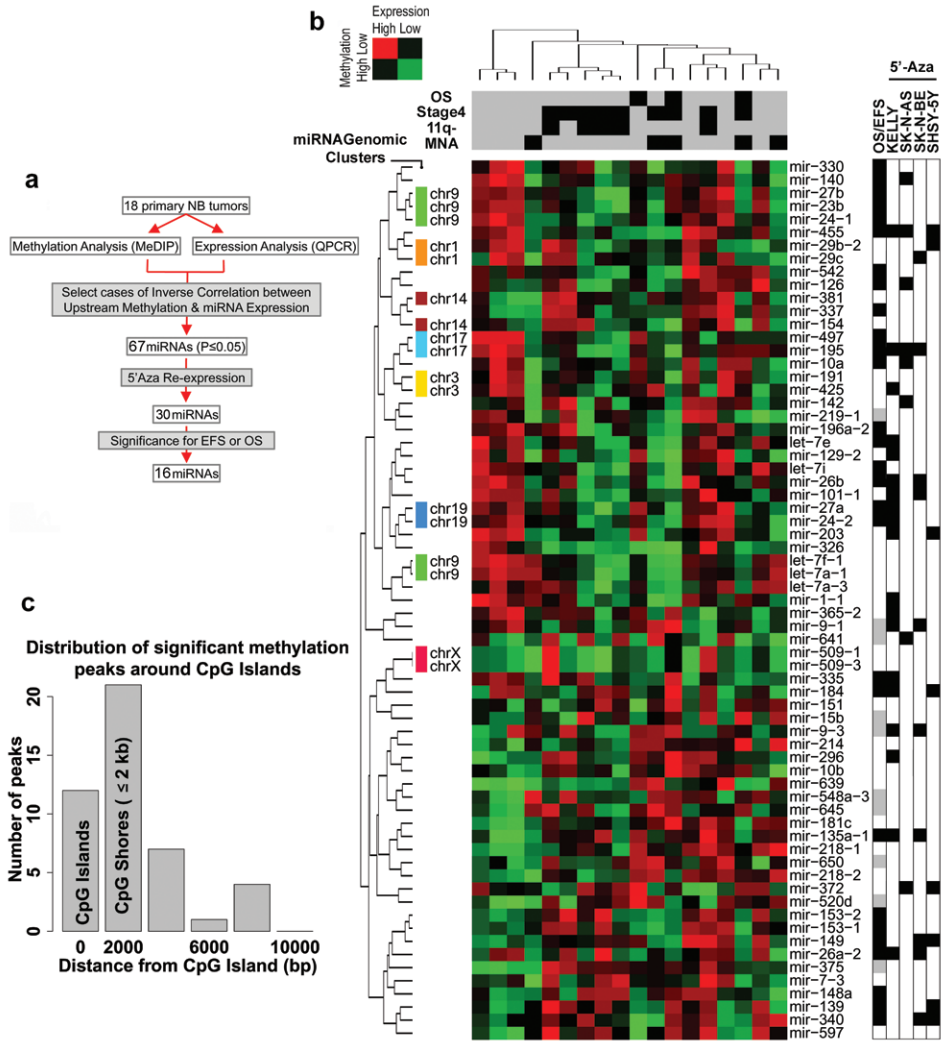


Figure 1. Identification of methylation sensitive miRNA
(a) Flowchart representing study design. **(b)** Integrated heatmap and two-dimensional hierarchical clustering for 67 methylation sensitive miRNAs. Tumors are clustered horizontally while miRNA are clustered vertically. Characteristics of the tumors are displayed at the top of the heat map. The heat map is based on both levels of miRNA expression and levels of DNA methylation at each locus, with a key to the color coding presented in the upper left corner. The colored vertical bar on the left designates miRNAs from the same cluster which display similarity in expression levels due to being under the control of a common upstream site of methylation. The table on the right designates miRNAs that are associated with poor OS/EFS when under-expressed in tumours (black, n = 28) or over-expressed in tumours (grey, n = 10). miRNAs that are up-regulated in response to the demethylating agent, 5-aza-cytidine, in four different cell lines are designated in the table. **(c)** The distribution of all methylation peaks within 10kb of CpG Islands. The majority of peaks occur within regions defined as CpG shores.

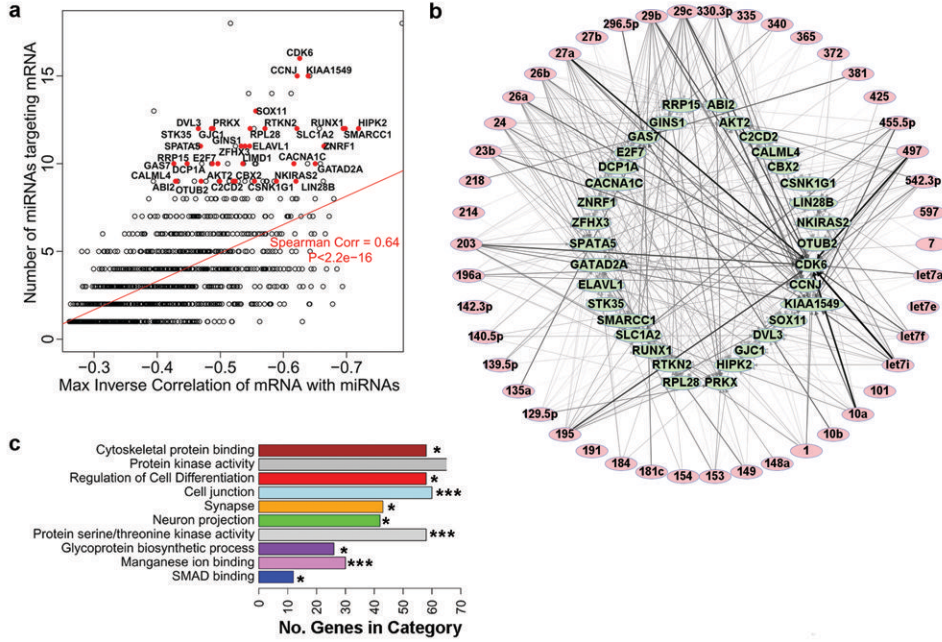


Figure 2. 3'UTR target analysis for methylation sensitive miRNA

(a) Scatter plot of the number of miRNAs predicted to target the mRNA (Y axis) vs. the maximum inverse correlation exhibited between the mRNA and miRNAs (X axis). Labeled mRNAs from the top 5% are significantly associated with poor OS when over-expressed in tumors. (b) A radial bipartite graph showing mRNAs highlighted in (a) with miRNA interactions. Only genes with significant associations with OS are depicted. Edge thickness is proportional to both inverse expression correlation and the over-representation of predicted mRNA targets. (c) Gene ontology analysis for the 1,250 over-represented target mRNAs with significant inverse correlation to the 67 methylation sensitive miRNAs. (*p<0.05; ** p<0.01, Benjamini corrected).

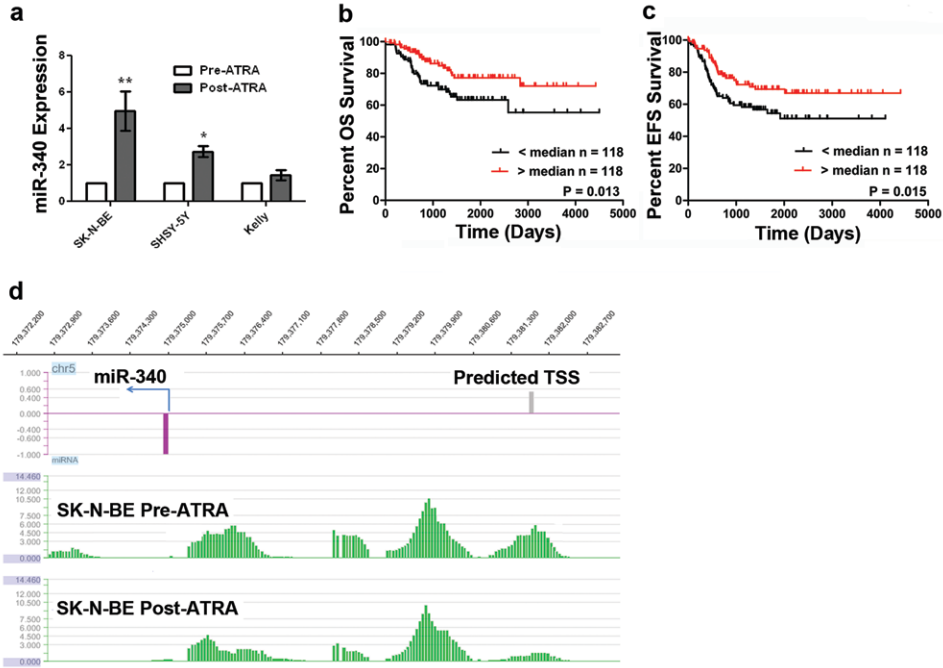


Figure 3. DNA methylation and expressional alterations of miR-340
(a) Relative expression of miR-340 in SK-N-BE and SHSY-5Y at 7 days post-ATRA. **(b,c)** Kaplan Meier survival plots for OS **(b)** and EFS **(c)** in 237 neuroblastoma tumors based on miR-340 expression. **(d)** SignalMap image from MeDIP analysis for the miR-340 upstream region. Only the methylation peak highlighted with a bracket (~6 Kb upstream) exhibited significant de-methylation in SK-N-BE cells 7 days post-ATRA. This peak overlaps the predicted TSS for miR-340. **(e)** Scatter plot of methylation vs. miR-340 expression in tumors showing a significant inverse correlation using Pearson’s correlation coefficient. **(f)** Expression of miR-340 following 5’-Aza-2 treatment of SK-N-BE and SHSY-5Y (*P <0.05; **P <0.01).

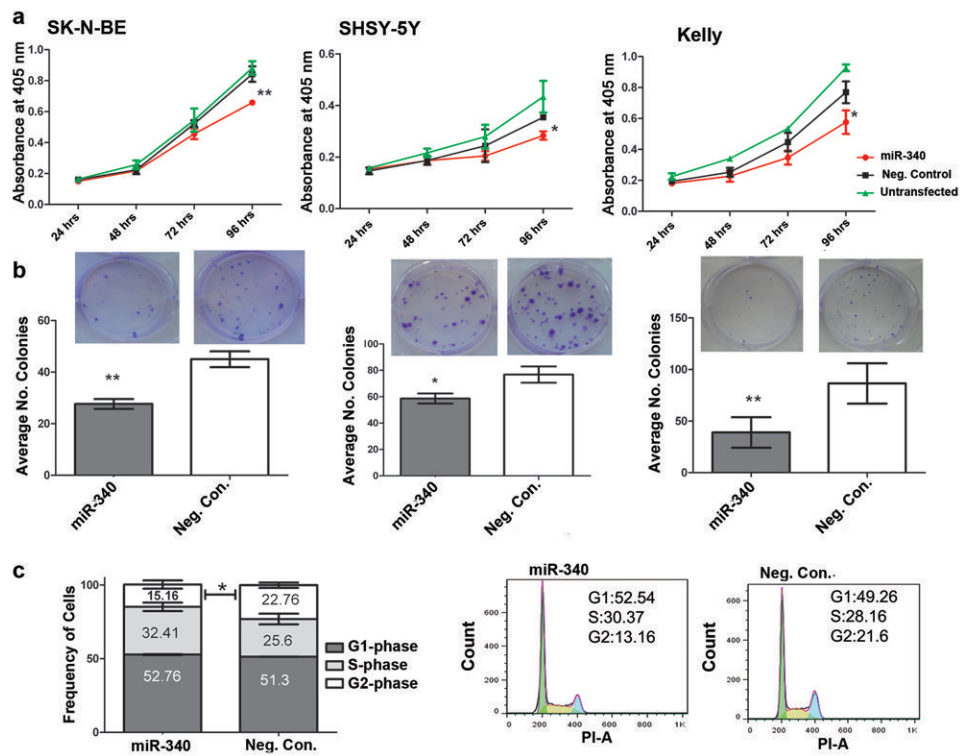


Figure 4. Functional effects of miR-340 on neuroblastoma cell lines
 (a) Cell viability assessment using an acid-phosphatase assay following transfection of miR-340 mimics or negative control into cells (*p<0.05; **p<0.01). (b) Clonogenic assays for each cell line transfected with either negative control or miR-340. Representative images are shown above each bar-graph. (c) Bar-graph represents the effects of miR-340 on cell cycle in SK-N-BE cells, as determined using PI-staining followed by FACS analysis. Each sub-section of the bars represents the percentage of cells in a distinct phase of the cell cycle. The histograms to the right of the bar-graphs are representative results.

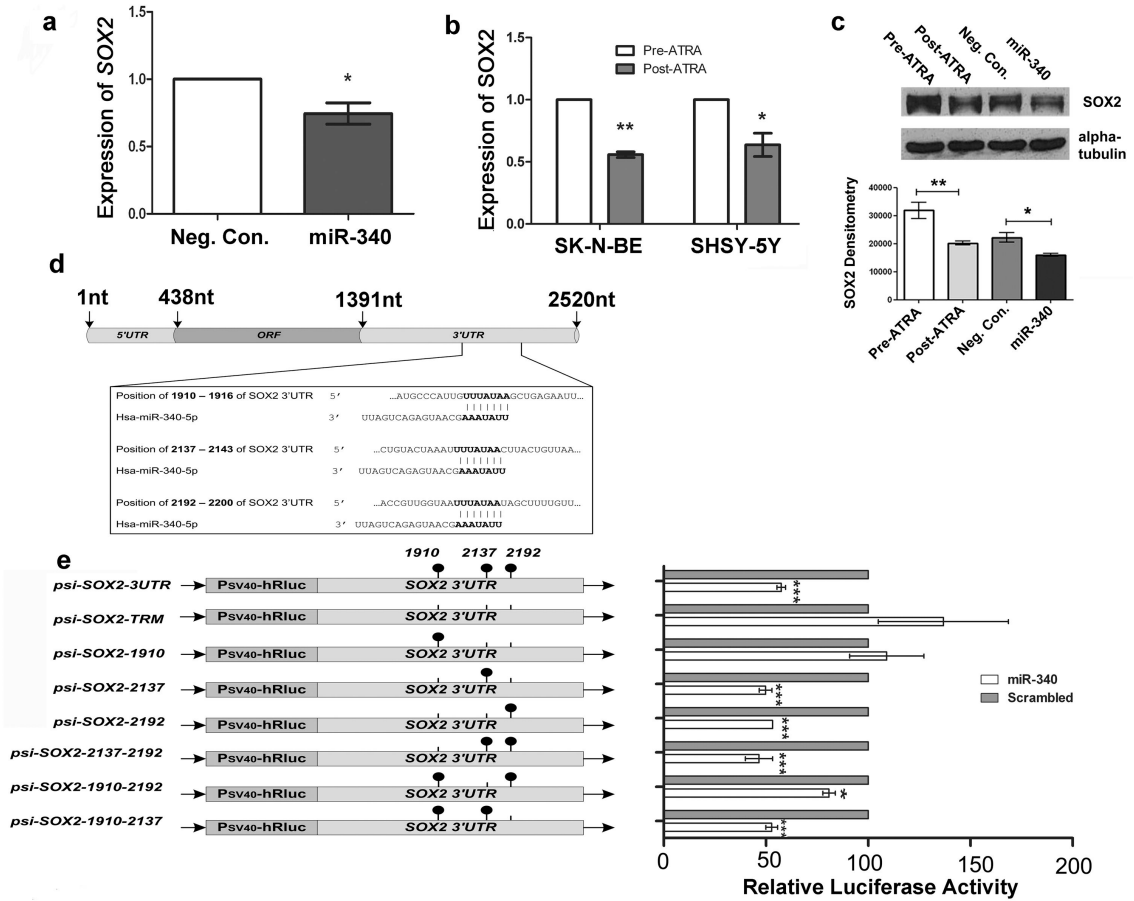


Figure 5. Analysis of SOX2 as a miR-340 target

(a) SOX2 mRNA levels assessed by TaqMan qPCR three days post-transfection of SK-N-BE cells with miR-340. (b) SOX2 mRNA levels in cells treated and untreated with ATRA for 7 days (c) SOX2 protein levels in miR-340 transfected SK-N-BE cells and in cells treated with ATRA. (d) Three distinct miR-340 target sites within the 1.1 kb 3'-UTR of SOX2 (TargetScan). The sites are designated 1910, 2137 and 2192 based upon the position of the first nucleotide of the seed site in the numbering of GenBank sequence NM_003106.3. (e) A panel of luciferase reporter plasmids with wild type and mutant target sites within the SOX2 3' UTR. psi-SOX2-3' UTR has the entire wild type 3'UTR; psi-SOX2-TRM is a triple deletion mutant for all three seed sites; double mutants are designated by the single site remaining active (e.g. psi-SOX2-1910 has the 2137 and 2192 seed regions deleted); and single mutants are designated by the two sites remaining active (e.g. psi-SOX2-2137-2192 has the 1910 seed site deleted). The bar graph demonstrates the effects on luciferase activity 48 hours after co-transfection of each construct with either miR-340 or a negative control. Renilla luciferase activity was normalized to fire fly luciferase (*p<0.05; **p<0.01; ***p<0.005).